Chinese Herbal Medicines 12 (2020) 36–46

Contents lists available at ScienceDirect

Chinese Herbal Medicines

journal homepage: www.elsevier.com/locate/chmed

Original Article

Mangiferin exerts neuroprotective activity against lead-induced toxicity and oxidative stress via Nrf2 pathway

Hao-wen Li[a,c,d,1], Tai-jin Lan[b,d,1], Chen-xia Yun[b,1], Ke-di Yang[c], Zheng-cai Du[d], Xue-fei Luo[e], Er-wei Hao[d], Jia-gang Deng[d,*]

[a] Community Health Services Management center, University of Chinese Academy of Sciences – Shenzhen Hospital, Shenzhen 518106, China
[b] School of Basic Medical Science, Guangxi University of Chinese Medicine, Nanning 530200, China
[c] MOE Key Lab of Environment and Health, Department of Occupational and Environmental Health, School of Public Health, Tongji Medical College, Huazhong University of Science and Technology, Wuhan 430030, China
[d] Guangxi Key Laboratory of Efficacy Study on Chinese Materia Medica, Guangxi University of Chinese Medicine, Nanning 530200, China
[e] Department of Clinical Laboratory, Ruikang Hospital Affiliated to Guangxi University of Chinese Medicine, Nanning 530011, China

ARTICLE INFO

Article history:
Received 5 May 2019
Revised 26 July 2019
Accepted 31 July 2019
Available online 14 December 2019

Keywords:
antioxidant
lead exposure
mangiferin
neuroprotective
Nrf2 pathway

ABSTRACT

Objective: The study was designed to assess the beneficial role of mangiferin (MGN) in lead (Pb)-induced neurological damages in the activation of Nrf2-governed enzymes, genes and proteins.

Methods: A total of 96 weaned Wistar rats (48 males and 48 females, 26- to 27-day-old), weighing 50–80 g were used. The experiment was performed in six groups: normal group (control, $n = 16$), model group (chronic Pb exposed, $n = 16$), Dimercaptosuccinic acid (DMSA)-treated group (positive control, Pb + DMSA, $n = 16$), three MGN-treated groups with different doses (Pb + MGN, $n = 48$). Normal group freely had access to purified water. DMSA-treated group was given DMSA, which was clinically used as the standard treatment for moderate Pb poisoning, at 50 mg/kg (2 mL suspension with purified water) by intragastric gavage (ig) 4 continual days a week for 4 weeks, MGN-treated groups were given MGN at 50, 100, or 200 mg/kg (2 mL suspension with purified water) by ig daily for 4 weeks. At the end of the treatment, all rats were sacrificed and the brain samples were collected. The haematoxylin and eosin (H&E) staining was used for observation of histopathology. Commercial kit, real-time quantitative polymerase chain reaction (RT-qPCR), Western-blot and immunohistochemistry (IHC) detection were used to detect the mRNA and protein expression.

Results: Eight weeks exposure to Pb-containing water resulted in pathological alterations, anti-oxidative system disorder in the brain, all of which were blocked by MGN in a Nrf2-dependent manner. Nrf2 downstream enzymes such as HO-1, NQO1, γ-GCS were activated. Nrf2, GCLC, GCLM, HO-1 mRNA and total Nrf2, Nuclear Nrf2, γ-GCS, HO-1 protein expression were affected too.

Conclusion: MGN ameliorated morphological damage in the hippocampus. Its neuroprotective effects were achieved by the activation of the Nrf2 downstream genes. The data from this *in vitro* study indicates that MGN targeting Nrf2 activation is a feasible approach to reduce adverse health effects associated with Pb exposure. Thus, MGN could be an effective candidate agent for the Pb-induced oxidative stress and neurotoxicity in the human body.

1. Introduction

Lead (Pb) is an environmental heavy metal pollutant that can enter the human or animals' body either through the digestive tract, respiratory tract or skin when contact with water, air or consume the contaminated foods (Nyqvist, Helmfrid, Augustsson & Wingren, 2017). Exposure to Pb may cause neurobehavioral damage to children (Martinez-Lazcano et al., 2018).

The developing nervous system is very sensitive to Pb-exposure (Singh et al., 2018). There have been many reports about the symptoms and mechanisms of Pb neurotoxicity. Lead impairs the neurological function through various means, among which

* Corresponding author.
E-mail address: dengjg@tom.com (J.-g. Deng).
[1] These authors contributed equally to this work.

https://doi.org/10.1016/j.chmed.2019.12.002

oxidative stress (OS) and cell apoptosis are the most popular and widely accepted mechanisms (Flora, Gupta & Tiwari, 2012; He, Poblenz, Medrano & Fox, 2000; Roy & Kordas, 2016). The use of appropriate pharmacological interventions that can effectively reduce oxidative stress has become an important strategy to prevent Pb-induced neurotoxicity.

Several studies have shown that the nuclear factor erythroid 2-related factor 2 (Nrf2) signaling pathway exerts neuroprotective effects by directly reducing oxidative stress (Ikram et al., 2019; Liu et al., 2018; Yang, Yu, Huang & Yang, 2019; Yao, Peng, Xu & Fang, 2019; Zhou et al., 2018). Nrf2 is a member of the transcription factor cap n' collar (CNC) family and was discovered and named by Moi in 1994 (Bock, 2012). It has been identified as a key regulator of the inducible expression of antioxidative enzymes and conjugation/detoxification proteins (Lou et al., 2019; Motohashi & Yamamoto, 2004; Scapagnini et al., 2011; Slocum & Kensler, 2011). In the central nervous system, Nrf2 activates genes such as heme oxygenase-1 (HO-1), quinone oxidoreductase 1 (NQO1), superoxide dismutase (SOD), glutathione peroxidase, thioredoxins, and glutathione S-transferase (GST) (Loboda, Damulewicz, Pyza, Jozkowicz & Dulak, 2016; Rubiolo, Mithieux & Vega, 2008; Sun et al., 2016; Thimmulappa et al., 2002). They participate in neuroprotection through their own properties (Haskew-Layton et al., 2010; Kwon et al., 2012; Yang et al., 2015). And the Nrf2 signaling pathway has been targeted for the Pb-induced neurotoxicity (Su et al., 2016; Wagner et al., 2017; Ye, Li, Li, Yuan & Chen, 2016).

Nowadays, numerous compounds from natural plants have been found to activate Nrf2 signaling pathway effectively (LGarcia-Nino & Pedraza-Chaverri, 2014; Liu et al., 2017; Su et al., 2016; Lu et al., 2018). Some phytochemical examples of Nrf2 stimulators include curcumin from turmeric (OoKhor, YingHuang, Limin-Shu & TonyKong, 2011), sulforaphane (SFN) from cruciferous vegetables (Jo, Kim, Kim, Park & Choi, 2014; Zhang, Su, Khor, Shu & Kong, 2013), epigallocatechin gallate (EGCG) from green tea (Han et al., 2014) and MGN (Mahalanobish, Saha, Dutta & Sil, 2019; Sadhukhan, Saha, Dutta & Sil, 2018; Xia et al., 2017). Thus, exploring more novel and effective candidate agents with low toxicity for Pb-induced neurotoxicity is essential and urgent.

Mangiferin (1,3,6,7-tetrahydroxyxanthone-C2-β-*D*-glucoside, MGN; Fig. 1A), or known as C-glucosyl xanthone, is predominantly found in the fruits, bark and leaves of *Mangifera indica* Linn (Wei, Deng & Yan, 2011). It exhibits wide range of pharmacological activities, including antioxidative, antitumor (Khurana, Kaur, Lohan, Singh & Singh, 2016), hepatoprotective (Saha, Rashid, Sadhukhan, Agarwal & Sil, 2016), immunomodulatory (Luczkiewicz, Kokotkiewicz, Dampc & Luczkiewicz, 2014), and so on (Dar et al., 2005; Duang, Wang, Zhou & Huang, 2011; Guha, Ghosal & Chattopadhyay, 1996). In the wide range of its beneficial activities, anticancer and antioxidant activities stand out as the prominent ones.

In addition, it protects against neuronal injuries, attenuates neurotoxicity, and increases neuronal survival in some cases *in vitro* (Peng, Hou, Yao & Fang, 2019). Some studies demonstrated that MGN was neuroprotective in pathological conditions (Wang et al., 2017) like ischemia *in vivo* (Gottlieb et al., 2006; Ibarretxe, Sanchez-Gomez, Campos-Esparza, Alberdi & Matute, 2006; Lemus-Molina, Sanchez-Gomez, Delgado-Hernandez & Matute, 2009; Yang, Weian, Susu & Hanmin, 2016). Moreover, MGN can improve spatial learning and memory in *D*-galactose-treated aging mice model (Pardo Andreu et al., 2010).

Several *in vivo* studies have shown that MGN plays an attenuative role in oxidative stress-mediated dysfunction via Nrf2 pathway (Zhang et al., 2015). *In vitro* studies have also shown that MGN protects against DNA damage via activating Nrf2 antioxidant response signaling pathway (Das, Ghosh, Roy & Sil, 2012). The neuroprotective effect of MGN was associated with attenuation of oxidant stress, enhanced translocation of Nrf2, and preservation of the activity of several antioxidant enzymes. However, there have been no reports on the neuroprotective effects of MGN on Pb-induced toxicities, and the underlying mechanism of its antioxidant properties is unclear.

In the current study, we established the Pb-exposure model, investigated the enzyme activities of Nrf2 downstream antioxidant enzymes, phase II enzymes (HO-1, NQO1, GST) and the GSH-related modulating enzyme (γ-GCS), their mRNA and protein expression, together with the neurological lesion to find out neuroprotective effects of antioxidant MGN in Pb-induced toxicity through the activation of Nrf2 signaling pathways. The results of this study will enhance understanding of the neuroprotective effects of MGN against Pb-induced toxicity and the underlying mechanisms, thereby supporting the use of this novel candidate agent for the prevention of Pb-induced toxicity.

2. Materials and methods

2.1. Reagents and materials

MGN was supplied by the Pharmaceutical Factory, Guangxi University of Chinese Medicine, (lot. 20081217, purity > 98%). DMSA was purchased from Sigma-Aldrich, Co., (lot 051M1275V).

A total of 96 weaned Wistar rats (48 males and 48 females, 26- to 27-day-old), weighing 50−80 g, obtained from Guangxi Medical University, Nanning, China were used in this study. Rats were housed in separate cages (four rats per cage) and kept on a 12:12-

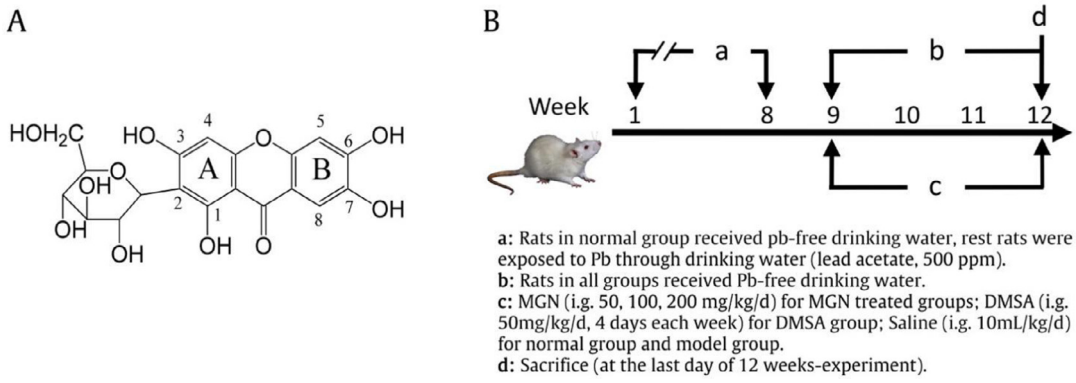

Fig. 1. Chemical structure of mangiferin (A) and treatment schedule (B) (MGN: mangiferin; DMSA: dimercaptosuccinic acid).

hour light/dark cycle with constant ambient humidity (50% ± 7%) and temperature [(25 ± 1) °C]. Water and food were available *ad libitum*. Experimental conditions and procedures involving animals were approved by Institutional Animal Ethics Committee (IAEC), Guangxi University of Traditional Chinese Medicine, and carried out in accordance with laboratory animal use guidelines of IAEC (Permit Number: SCXK (GUI) 2009-0002). Animal handling followed the National Animal Welfare Law of China.

2.2. Treatment schedule

The experiment was performed in six groups of weaned Wistar rats (postnatal days 26–27, male and female, weighing 50–80 g): normal group (control, $n = 16$), model group (chronic Pb exposed, $n = 16$), DMSA-treated group (positive control, Pb + DMSA, $n = 16$), three MGN-treated groups with different doses (Pb + MGN, $n = 48$).

At the very beginning of the experiment, 96 rats were randomly assigned into two parts, of which 16 rats (8 males and 8 females) were in the first part, they were in the normal group (blank control). And the rats freely had access to purified water. There is no Pb exposure throughout the lifetime in the normal group.

The remaining 80 rats in the second part freely had access to purified water with lead acetate (Pb Ac500 ppm). After the 8 weeks' Pb exposure, second part rats were divided into the other five groups based on their body weight, each group consisted 16 rats (8 males and 8 females), which were model group, DMSA-treated group, and three MGN-treated groups. DMSA-treated group was given DMSA at 50 mg/kg (2 mL suspension with purified water) by ig 4 continual days a week for 4 weeks; MGN-treated groups were given MGN at 50, 100, or 200 mg/kg (2 mL suspension with purified water) by ig daily for 4 weeks.

Determination of the dose was based on literatures (Li et al., 2013; Pal, Sinha & Sil, 2013). Saline was administered to the normal group and model group daily according to the same volume as that of MGN-treated groups. The treatment schedule was shown in Fig. 1B.

2.3. Sample collection

At the end of the experiment, all experimental rats were sacrificed, three male and three female rats randomly selected in each group were given cardiac perfusion with a solution of 4% paraformaldehyde-1% glutaraldehyde in 0.1 mol/L phosphate buffer, the brains were resected immediately from the skull as soon as the color of the heart turns white, and then fixed overnight by perfusing with 4% paraformaldehyde and subsequently embedded in paraffin for H&E stainning and immunohistochemistry (IHC) test; The brains of the rest 10 rats in each group were resected directly and kept at −80 °C until biochemical determination, real-time quantitative PCR and Western blot analysis.

2.4. Histological examination

After cardiac perfusion, the brains were used to make paraffin section. Samples were removed from the hippocampal CA1 area. A transverse section of 4 mm thick was cut from each sample and stained with H&E staining using the standard protocol.

2.5. Biochemical determination

In the brain homogenate, the activities of antioxidant enzymes which included catalase (CAT), superoxide dismutase (SOD), glutathione reductase (GR), glutathione peroxidase (GSH-PX), and γ-glutathione-S transferase (GST), were assayed using commercial assay kits (Jiancheng Bioengineering Institute, Nanjing, China). The content of oxidized glutathione (GSSG) and GSH, malondialdehyde (MDA), and hydrogen peroxide (H_2O_2) was also measured using commercial assay kits.

The inhibition of nitroblue tetrazoliu (NBT) reduction by the xanthine/xanthine oxidase system to generate O^{2-} was used to measure the total SOD activity in the brain homogenate. One SOD activity unit was defined as the amount of enzyme causing 50% inhibition in 1 mL reaction solution and the result expressed as units per mgprot (milligram protein). CAT activity in the brain homogenate was detected using the ammonium molybdate method by measuring the intensity of a yellow complex formed by molybdate and H_2O_2 at 405 nm, after ammonium molybdate was added to terminate the H_2O_2 degradation reaction catalyzed by CAT. An enzyme activity unit was defined as the degradation of 1 mmol H_2O_2 per second per milligram brain homogenate; It was expressed as units per milligram protein. GSH-Px activity was measured by quantifying the rate of H_2O_2-induced oxidation of GSH to GSSG under the existence of GSH-Px based on the modified method of 5,5-dithiobis-2-nitrobenzoic acid (DTNB). GR activity was determined by measuring the rate of NADPH oxidation as a result of absorbance reduction at 340 nm. One unit of GR activity was defined as 1 g brain homogenate which consumed 1 mmol NADPH at 340 nm for 1 min. The activities of GR were expressed as units per gprot (gram protein). H_2O_2 in the brain homogenate was detected by measuring the intensity of a yellow complex formed by molybdate and H_2O_2 at 405 nm. The total levels of GSSG and GSH were measured using the colorimetric microplate assay kits by DTNB-GSSG recycling assay method. The total GSH assay after the brain homogenate was pretreated with 1% 1 mol/L 2-vinylpyridine solution to eliminate the reduced GSH, which was obtained by subtracting the amount of GSSG from the total GSH. The content of H_2O_2 was expressed as units per gram brain homogenate.

Concentration of MDA was determined using the thiobarbituric acid (TBA) method. A pink chromogen compound which absorbance at 532 nm was formed as a result of combination of the MDA and TBA determined the amount of LPO which was expressed as nanomoles per milligram protein. All spectrophotometric measurements were carried out in a multifunctional microplate-based spectrophotometric reader (Epoch Multi-Volume Spectrophotometer System, USA).

NQO1 activity was detected using NQO1 detection kit (ELISA) (Catlog NO.: CSB-EL015671RA, Cusabio Biotech Co., Ltd. Wuhan, China). It was measured as 2,6 -dichloro-indophenol reaction system a second electron acceptor. A total of 5 μL protein was added into 0.9 mL reaction buffer (containing 50 mmol/L Tris–HCl (pH 7.5), 0.25 mmol/L NADPH, 80 μmol/L DCIP). The tests of enzyme activities were carried out for 3 min at 405 nm, and the enzyme activity unit was defined as the decrease of absorbance value per minute per milligram.

HO-1 activity was tested using HO-1 ELISA detection kit (Catalog No.: CSB-EL8742RA, Cusabio Biotech Co. Ltd. Wuhan, China). The HO-1 content was calculated according to the HO-1 protein standard curves with OD value of sample at 450 nm.

2.6. Real-time quantitative PCR

Real-time quantitative polymerase chain reaction (PCR) was performed to determine the mRNA levels of Nrf2, GCLC, GCLM, and HO-1. The total RNA was isolated from brain using a commercial kit (AxyPrep^{TM} Total RNA MiniPrep Kit; Axygen Biotechnology, Hangzhou, China) in accordance with the manufacturer's instructions. RNA purity was tested with BioPhotometer (Eppendorf, Germany), which showed an optical density ratio (OD_{260}/OD_{280})

that was between 1.8 and 2.0. First-strand cDNA was synthesized (RevertAid^{TM} First Strand cDNA Synthesis Kit; Fermentas, Lithuania). Real-time RT-PCR was performed with an ABI PRISM 7900HT Sequence Detection System (Applied Biosystems, USA) using Platinum SYBR Green qPCR SuperMix-UDG (Invitrogen, USA). GAPDH was used in parallel for each run as internal control. A 10 μL PCR reaction system which included the appropriate cDNA concentration of 0.5 μL, 0.3 μL forward and reverse primers (10 μmol/L), SuperMix 5 μL, and 3.9 μL DEPC-treated H_2O were used. A four-step experimental run protocol was carried out with the following amplification conditions, initial denaturation for 10 min at 95 °C; followed by 40 cycles of denaturation for 15 s at 95 °C and 1 min of elongation at 60 °C. A melting curve was generated at the end of every run to ensure product uniformity (95 °C for 15 s, 60 °C for 15 s, 95 °C for 15 s). The relative expression of target genes (Nrf2, GCLC, GCLM, HO-1) was calculated using $2^{-\triangle\triangle Ct}$. The primer sequences were designed according to cDNA sequence from GenBank (Table 1) and synthesized by the Sangon Biotech (Shanghai, China).

Table 1
Description of primers used in present study.

Primers	Types	Primer sequences	Length/bp
Nfe2l2	Forward	ATTGCCACCGCCAGGACTAC	310
Nfe2l2	Reverse	AATGTGGGCAACCTGGGAGT	
Hmox1	Forward	CGGAGCCAGCCTGAACTAGC	193
Hmox1	Reverse	CAAGGAGGCCATCACCAGCTTA	
Gclc	Forward	CAAGTGGGGTGACGAGGTGG	257
Gclc	Reverse	CCTCCTTCCGGCGTTTCCTC	
Gclm	Forward	AGACCGGGAACCTGCTCAAC	75
Gclm	Reverse	AGTCTCGAAGCTCCTCGCTGT	
GAPDH	Forward	GCACCGTCAAGGCTGAGAAC	138
GAPDH	Reverse	TGGTGAAGACGCCAGTGGA	

2.7. Western blot

Brain homogenate were prepared in lysis buffer (1 mmol/L phenylmethylsulfonyl fluoride, 2 mmol/L EGTA, 10 mmol/L EDTA, 20 mmol/L Tris–HCl (pH 7.4), 100 mmol/L PMSF, 250 mmol/L sucrose, and 0.1% Triton X-100 to detect protein of Nrf2, GCLC, GCLM, and HO-1. Each protein sample was measured by Protein Assay Kit (Bio-Rad, Hercules, CA). Equivalent amounts proteins (60 μg) were separated in 10% SDS-polyacrylamide gel and transferred electrophoretically onto a PVDF membrane. The membranes were blocked in TBST containing 5% non-fat dry milk (w/v), and then incubated at 4 °C overnight with rabbit anti-HO-1 (Santa Cruz Biotechnology, USA, sc-1796) at a 1:200 dilution, anti-γ-GCS (Santa Cruz Biotechnology, Inc., USA, sc-22755) at a 1:500 dilution, anti-Nrf2 (Santa Cruz Biotechnology Inc., USA, sc-722) at a 1:100 dilution or anti-β-actin (Santa Cruz Biotechnology Inc., USA, sc-47778) at 1:2000 dilution. After being washed with TBST buffer, membranes were incubated for 2 h at 37 °C with the secondary antibody conjugated to horseradish peroxidase (Santa Cruz Biotechnology Inc., USA, sc-2004) diluted at 1:5000. Subsequently ECL Western blot detection system Image Station 4000 MM (KODAK Digital Imaging System) was used to detect immune-reactive protein and densitometric analysis of immunoblots was performed with Gel pro 3.0 software.

The cytoplasmic protein and nuclear protein were extracted according to instructions of Cytoplasmic and Nuclear Protein Extraction Kit (Beyotime Biotech Inc., Nantong, China) to measure the Nrf2. Equal amounts of protein were subjected to SDS-polyacrylamide gel and transferred electrophoretically onto a PVDF membrane as described above. The membranes were incubated with primary antibody for Nrf2 (Santa Cruz Biotechnology Inc., USA, sc-722) at a 1:100 overnight at 4 °C. The next day, the membranes were then washed in PBS and incubated for 1 h at room temperature with the secondary antibody conjugated to horseradish peroxidase (Santa Cruz Biotechnology Inc., USA, sc-2004) diluted at 1:5000. Subsequently ECL Western blot detection system Image Station 4000 MM (KODAK Digital Imaging System) was used to detect immune-reactive protein and densitometric analysis of immunoblots was performed with Gel pro 3.0 software.

2.8. Immunohistochemistry

Non-biotin two-step technique was used for IHC detection. It allowed small monomer organic molecules coupling the rabbit immunoglobulin and peroxidase to the multimeric form to allow each antibody to attach to multiple enzymes. It replaced the secondary antibody in traditional method, amplified the antigen-antibody binding signal, and fixed the antigens in tissue sections and smears. The primary antibody employed was rabbit anti-Nrf2 (Santa Cruz Biotechnology Inc., USA, sc-722). Two-Step IHC Detection Reagent (PV-6001) was obtained from Beijing Zhongshan Golden Bridge Company (Beijing, China). Dilution of the rabbit polyclonal primary anti-Nrf2 antibody was 1:50, and the goat anti-rabbit secondary antibody was 1:500. Negative controls were processed simultaneously by substituting primary antibodies with normal IgG at the same dilution. Slides processed without primary antibodies served as negative controls. Slides were observed under a digital camera linked microscope (Olympus, Japan) and photos were taken. Each slice was divided into multiple potential regions of interest, and five non-overlapping regions were randomly selected under 200× magnifications, with consistent brightness. Five slides were prepared for each experiment group.

2.9. Statistical analysis

All statistical analysis was performed using the software Package for Statistical Analysis (SPSS), version 16.0 (SPSS Inc., USA). Data were presented as mean ± S.D. The significance of variables among groups was analyzed using ANOVA, and a post hoc test was performed when necessary. P values of <0.05 were considered statistical significance in this study.

3. Results

3.1. Effects of MGN on hippocampal histological changes in experimental rats

The changes shown in the brain of model group included neuropile vacuole, abnormal dense bodies in cytoplasm and lysosome in the peripheral vessels, and pyknotic compact of gliocyte. In the DMSA-treated group, morphological changes were similar to the model group, such as apoptotic cell with pyknotic nuclei containing small, dispersed chromatin clumps, necrotic cells with a lack of identifiable nuclear membranes ultrastructure, and cytoplasmic vacuoles were frequently observed. While in the MGN-treated groups, the anomaly was mild and the cells in the CA1 area in hippocampus were almost normal (Fig. 2). The histological examination of the hippocampus revealed that MGN had protective effect against Pb-induced toxicity and DMSA did not show that effect. The morphological images of hippocampal areas CA1 in the control and experimental animals were coincident with our preliminary work by Transmission electron microscopy (TEM) (Li et al., 2013).

3.2. Effects of MGN on MDA, H_2O_2 content and SOD, CAT activities in brain of experimental rats

CAT and SOD are two key enzymes in detoxifying intracellular O^{2-} and H_2O_2. As shown in Fig. 3, SOD activity was increased significantly in the brain homogenate at the dose of 100 mg/kg and 200 mg/kg but not at the dose of 50 mg/kg in MGN-treated groups. And CAT activity was increased significantly in all MGN-treated groups. The concentrations of MDA and H_2O_2 were increased in the model group when compared with that in the normal group, while the concentrations of MDA and H_2O_2 were significantly decreased in MGN-treated groups at the doses of 100 mg/kg and 200 mg/kg when compared with the model group. Moreover, both SOD and CAT activities were significantly increased in

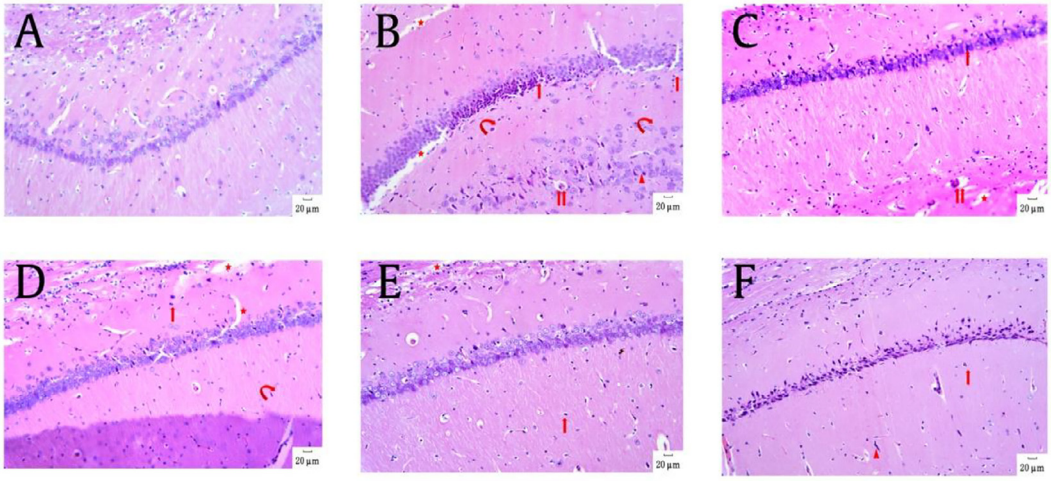

Fig. 2. Effects of MGN on lead-exposed hippocampal histological changes in experimental rats. (H&E staining, magnification 200×, scale bars = 20 μm, only a representative picture was shown for each group). (A) Normal; (B) model; (C) DMSA; (D) MGN 50 mg/kg; (E) MGN 100 mg/kg; (F) MGN 200 mg/kg.
(A) Normal group showing neurons with large, rounded or ovoid, open face nuclei and normal distribution of cytoplasm. (B) and (C) Lead-exposed group and DMSA-treated group showing pyknotic compact (triangle) of gliocyte, edema, congestion (circle arrow), perivascular and pericellular spaces (star), neuropile vacuole, abnormal dense bodies (double arrow) in cytoplasm and lysosome in the peripheral vessels. Apoptotic cell with pyknotic nuclei containing small, dispersed chromatin clumps, necrotic cells, and cytoplasmic vacuoles were observed. (D), (E) and (F) MGN-treated groups showing mild anomaly and the cells in the CA1 area in hippocampus were similar to that in normal group.

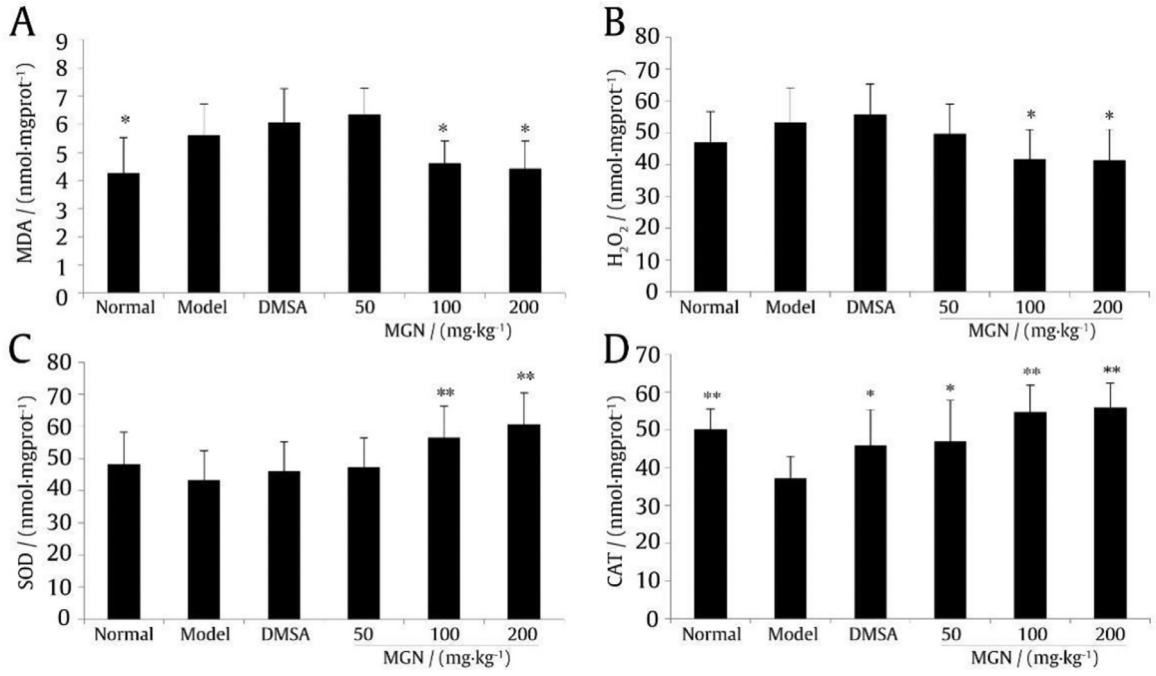

Fig. 3. Effects of MGN on content of MDA (A) and H_2O_2 (B) and activities of SOD (C) and CAT (D) in brain of experimental rats (means ± SD, $n = 10$). $^{*}P < 0.05$; $^{**}P < 0.01$ *vs* model group.

MGN-treated group at the dose of 200 mg/kg. when compared with the model group, the concentrations of MDA and H_2O_2 were increased and SOD and CAT activities were increased in DMSA-treated group, but the increase of SOD activities were not statistically significant.

3.3. Effects of MGN on GSH, GSSG content and GSH/GSSG ration in brain of experimental rats

GSH is well known for its antioxidant role in the central nervous system (CNS). GSH not only scavenges multiple oxidative species such as hydroxyl radical, NO and superoxide (Aoyama, Watabe & Nakaki, 2008); it also serves as a reservoir for cysteine to protect against toxicity secondary to high cysteine concentrations (Janaky, Varga, Hermann, Saransaari & Oja, 2000). GSH content significantly increased, but GSSG content did not significantly changed in MGN-treated groups and DMSA-treated group, and the GSH/GSSG ratio was increased in a dose dependent fashion (Fig. 4).

3.4. Effects of MGN on activity of phase II enzymes: GST, HO-1 and NQO1 in brain of experimental rats

GST is an abundant protein that has a number of iso-enzymes, it conjugates GSH to electrophiles and xenobiotics (Raza, 2011) and some of their isoenzymes participate in neuroprotection. HO-1 and HO-2 are two isoforms of active heme oxygenase (HO). HO-1 belongs to the phase II enzymes and only expresses in an inducible manner. HO-1 plays an important role in neuroprotection by breaking down heme to protect cells through a net reduction in superoxide and other ROS as well as by generation of antioxidants. NQO1, also named DT-diaphorase, uses either NADPH or NADH as the hydride donor to catalyze the two electrons reduction of quinone to the redox-stable hydroquinone, thus preventing free radical formation from quinone derivatives (Talalay, Fahey, Holtzclaw, Prestera & Zhang, 1995). In our study, the GST, HO-1 and NQO1 activities were significantly increased in MGN-treated groups. While in DMSA-treated group, the activities of GST, HO-1 and NQO1 were increased, but the increase of the HO-1 and NQO1 activities were not statistically significant (Fig. 5).

3.5. Effects of MGN on activities of GSH related enzymes: γ-GCS, GSH-Px and GR activity in brain of experimental rats

The synthesis of GSH requires the consecutive action of enzyme glutamate cysteine ligase GSH-Px (GCL; also known as γ-glutamylcysteine synthetase, γ-GCS) and GSH synthetase. It is the rate-limiting step in GSH biosynthesis. Glutathione peroxidase (GSH-Px) is a specific enzyme that mediated the transfer of GSH to its substrates (Cho, Reddy, Debiase, Yamamoto & Kleeberger, 2005). In the model group, the GSH related enzymes' activities were significantly decreased. The activity of γ-GCS was significantly increased in MGN-treated groups, especially at the dose of 100 and 200 mg/kg. The activity of GSH-Px was significantly increased at the dose of 100 mg/kg and 200 mg/kg in MGN-treated groups, while GR activity did not significantly change in MGN-treated groups (Fig. 6). Their activities were increased but not statistically significant in DMSA-treated group.

3.6. Effects of MGN on Nrf2, GCLC, GCLM, HO-1 mRNA expressions in brain of experimental rats

The antioxidant/phase II detoxifying enzymes and GSH-related enzymes were increased in MGN-treated group. As all of these enzymes are governed by Nrf2, we tested GCLC, GCLM, and HO-1 to assess the effect of MGN on Nrf2-regulated gene. The mRNA levels of Nrf2 in rat brain homogenate were determined by real-time quantitative PCR. The enzyme GCL is the downstream gene of Nrf2, catalyzes the rate-limiting step of glutathione synthesis. Its holoenzyme is composed of a catalytic (GCLC) and a modifier (GCLM) subunit. Not only GCL, in this part, another downstream gene of Nrf2, namely HO-1 was also determined. Fig. 7(A) indicated that the levels of Nrf2 mRNA were increased in both model and MGN-treated groups but not statistically significant ($P > 0.05$), and that remained unchanged in DMSA-treated group ($P > 0.05$). As indicated in Fig. 7B and C, mRNA expressions of GCLC and HO-1 were inhibited in model group, while in MGN-treated groups, they were improved significantly ($P < 0.05$) in a dose-dependent manner. GCLC mRNA expression was remained unchanged and HO-1 mRNA expression was increased in DMSA-treated group. No difference was shown in GCLM mRNA expression among the six groups.

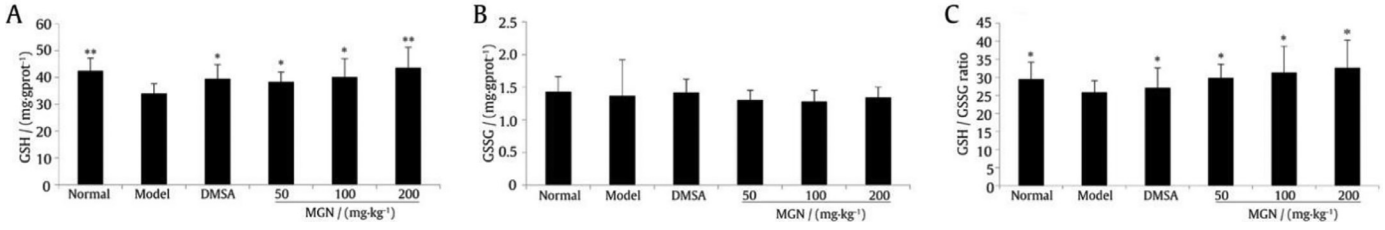

Fig. 4. Effects of MGN on activities of GSH (A) and GSSG (B) and GSH/GSSG ration (C) in brain of experimental rats (means ± SD, $n = 10$). $^{*}P < 0.05$; $^{**}P < 0.01$ *vs* model group.

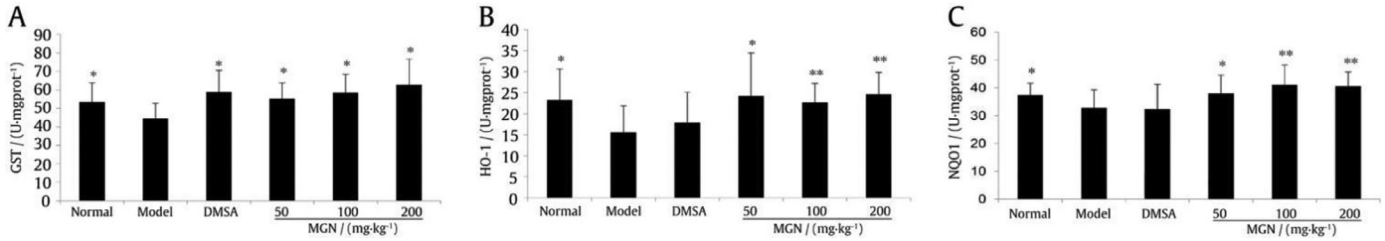

Fig. 5. Effects of MGN on activities of phase II enzymes GST (A), HO-1(B) and NQO1 (C) in brain homogenate of experimental rats (means ± SD, $n = 10$). $^{*}P < 0.05$; $^{**}P < 0.01$ *vs* model group.

3.7. Effects of MGN on total Nrf2, nuclear nrf2, γ-GCS, HO-1 protein expression in brain of experimental rats

The expression of Nrf2 protein in nuclear and cytoplasmic extracts were analyzed by Western blot. As shown in Fig. 8A and B, Nrf2 in normal group, were nearly undetectable in the cytoplasmic and nuclear extract, respectively. Upon treatment with MGN, Nrf2 protein was rapidly accumulated in the nucleus. Nrf2 expression was increased insignificantly in DMSA-treated group. γ-GCS and HO-1 were subjected to regulation by Nrf2, as indicated in Fig. 8C

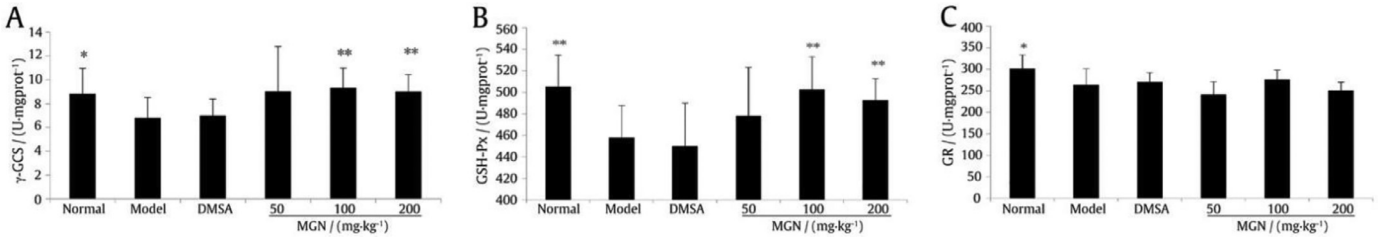

Fig. 6. Effects of MGN on activities of GSH related enzymes γ-GCS (A), GSH-Px (B) and GR (C) in brain of experimental rats (means ± SD, $n = 10$). $^{*}P < 0.05$; $^{**}P < 0.01$ *vs* model group.

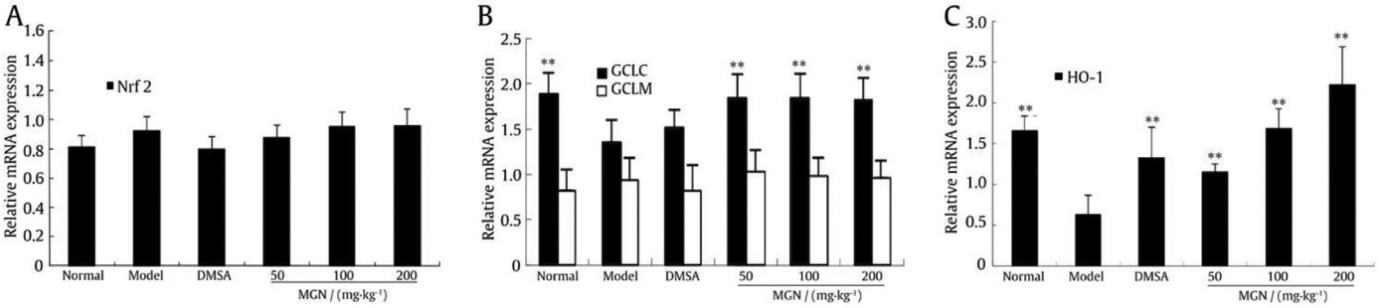

Fig. 7. Effects of MGN on Nrf2 (A), GCC and GCLM (B), and HO-1 (C) mRNA expression in brain of experimental rats (means ± SD, $n = 10$). $^{*}P < 0.05$; $^{**}P < 0.01$ *vs* model group.

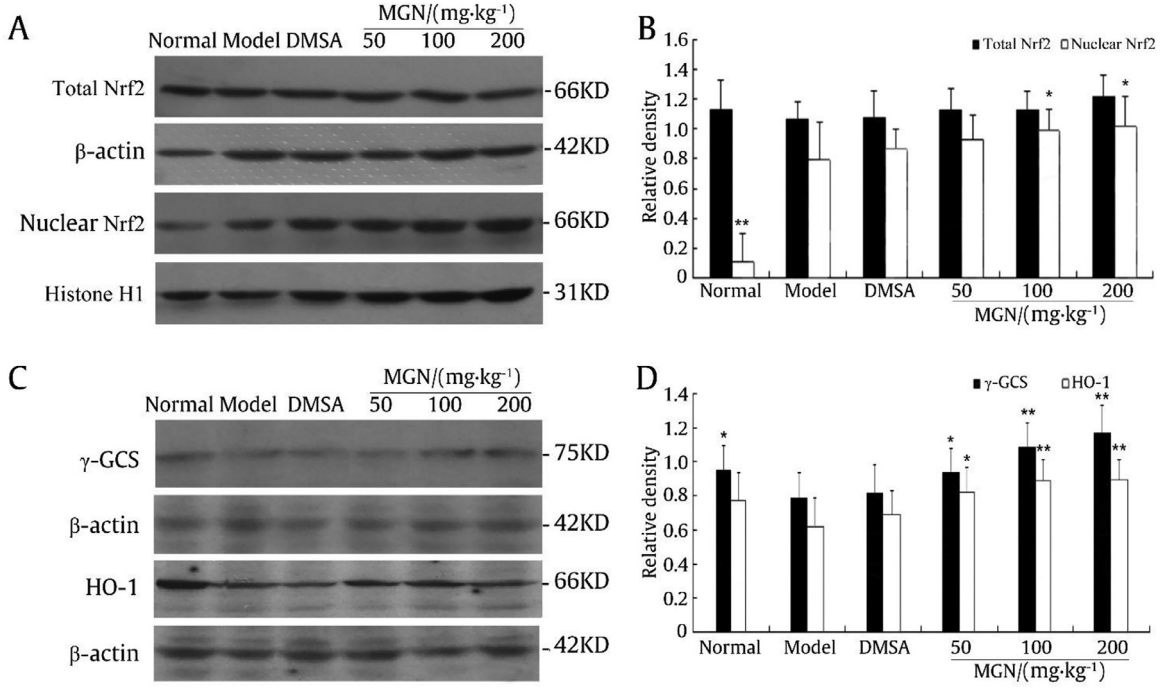

Fig. 8. Effects of MGN on total Nrf2, nuclear nrf2, γ-GCS and HO-1 protein expression in brain of experimental rats. At the last day of experiment, 10 rats in each group were sacrificed and then their brains were collected as described in Materials and Methods. (A) The levels of total Nrf2 and nuclear nrf2 in brain tissues were measured by Western blot. (B) Bar plot of the average relative density of total Nrf2 and nuclear nrf2. (C) The levels of γ-GCS and HO-1 in brain tissues were measured by Western blot. (D) Bar plot of the average relative density of γ-GCS and HO-1. Only a representative picture is shown for each group. Values shown were percent of β-actin control band except for nuclear Nrf2 protein, and histone 1 as the control band for nuclear Nrf2 protein. The data are representative of three independent experiments and represented as the means ± SDs ($n = 10$). $^{*}P < 0.05$; $^{**}P < 0.01$ *vs* model group.

and D, γ-GCS, HO-1 were significantly decreased in model group, significantly increased in all MGN-treated groups but remained unchanged in DMSA-treated group.

3.8. Effects of MGN on Nrf2, γ-GCS protein expression shown by IHC detection in brain of experimental rats

In IHC detection results, most of the Nrf2-positive cells were detected in MGN-treated groups, a few of Nrf2-positive cells were detected in model group and DMSA-treated group, and no Nrf2-positive cells were detected in normal group (Fig. 9). Besides, we found that γ-GCS positive cells in the model group were lesser than that in the normal group, but increased in DMSA-treated group, and significantly increased in MGN-treated groups (Fig. 10).

4. Discussion

Current data indicated that low-level exposures to Pb, may cause cognitive dysfunction, neurobehavioral disorders, and neurological damage (Nyqvist et al., 2017). As a means of reducing the body Pb burden, chelation therapy has been used for more than half a century (Sakthithasan, Levy, Poupon & Garnier, 2018). However, it is not well known whether chelation therapy is equally effective in the recovery of altered neurological disorders as they were hampered in removing Pb from brain and skeleton (Flora, Saxena, & Mehta, 2007). Nowadays, one of the aims of the treatment of Pb-toxicities is to prevent the oxidation-related disease (Gurer & Ercal, 2000; Patrick, 2006). The agents that can relieve oxidative stress related pathological lesions are urgently needed. Various herbal medicines and diet-derived natural products with properties such as antioxidation (Winiarska-Mieczan, 2018), Nrf2 inducer, could be the suitable candidates for this purpose.

In our study, the Pb-exposed animal model was established in weaned Wistar rats by exposing to 500 ug/mL of lead acetate in the drinking water. DMSA (also called succimer), which has been approved as the standard treatment for moderate Pb poisoning (2017) was used as the positive control in our study.

Lead toxicity affects the central and peripheral nervous systems (Vorvolakos, Arseniou & Samakouri, 2016), our results showed that two months' exposure to Pb resulted in substantial pathological changes in the hippocampus and cerebral cortex of model group (Fig. 2). It was reported that the GSH metabolism and GSH related enzymes such as GR, GSH-Px were affected when MDA occurred in occupationally-exposed workers (Hsu & Guo, 2002; Lopes, Peixe, Mesas & Paoliello, 2016). Consistent with these studies, our results showed the decrease of the levels of CAT, GSH-Px, GR, GST, GSH, SOD, GSH/GSSG ratio, and the increase of the levels of MDA and H_2O_2 in the brain homogenate of the model group (Figs. 3–6). These results suggested that the body system was beginning to lose its ability to maintain the critical balance of the redox states after two months exposure to the lead acetate treated drinking water.

It has been demonstrated that Nrf2 activation is effective in preventing oxidative stress related pathogenesis (Wang et al., 2019). Under basal conditions, cells mediate the constant degradation of Nrf2 through the ubiquitin proteasome systems (UPS), keeping Nrf2 protein levels low and preventing transcription of unneeded genes (Harder et al., 2015). Upon activation, Nrf2 accumulates in the nucleus, where it formed to be a hetero-dimer with small Maf proteins. These Nrf2-Maf heterodimers recognize antioxidant response elements (AREs), 11-(or16) bp enhancer sequences in the regulatory region of Nrf2 target genes, thereby allowing the recruitment of key factors for transcript synthesis (Hayes, McMahon, Chowdhry & Dinkova-Kostova, 2010).

Up-regulation of this series of Nrf2-target genes helps the cell to combat harmful stressors such as reactive oxygen species (ROS) and electrophilic xenobiotics, effectively providing a cellular survival mechanism. This cytoprotective activity of Nrf2 has been implicated in disease prevention, including neuroprotection (Ikram et al., 2019; Yao et al., 2012).

Several studies have shown that phytochemical MGN is a Nrf2 inducer, Its neuroprotective effects were achieved via activating Nrf2/ARE antioxidant response signaling pathway (Das et al., 2012; Zhang et al., 2015). Therefore, in this study, we examined the histological lesions, investigated the enzyme activities of Nrf2 downstream antioxidant enzymes, phase II enzymes (HO-1, NQO1, GST) and the GSH-related modulating enzyme (γ-GCS), together with the mRNA and protein expression, Nrf2 translocation, to find out protective effects of antioxidant MGN in Pb-induced toxicity, and its activation on Nrf2 signaling pathways.

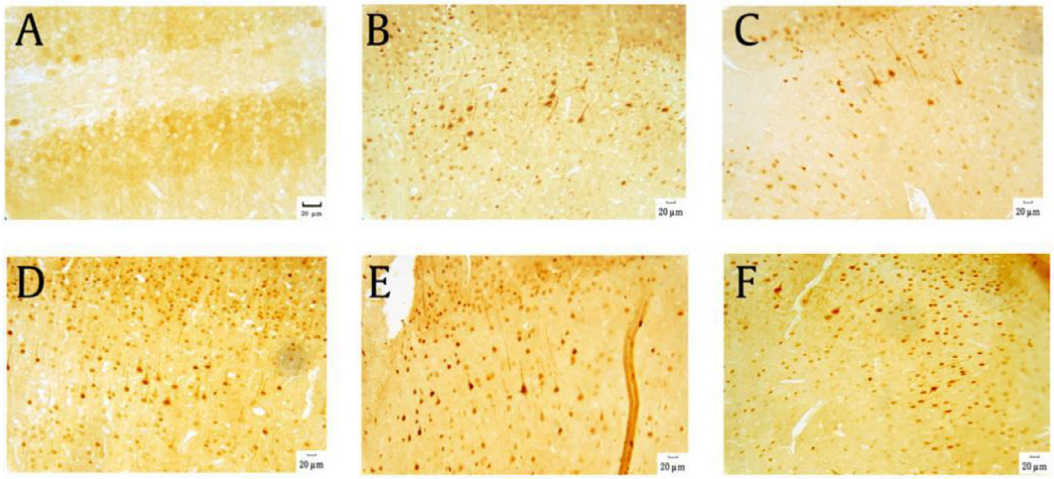

Fig. 9. Effects of MGN on Nrf2 protein expressions shown by IHC detection in brain of experimental rats. (A) Normal; (B) Model; (C) DMSA; (D) MGN 50 mg/kg; (E) MGN 100 mg/kg; (F) MGN 200 mg/kg. At the last day of experiment, three male and three female rats randomly selected in each group were sacrificed and then their brains were collected as described in Materials and Methods. The expression of Nrf2 in brain tissues was detected by IHC (magnification 200×, scale bars = 20 μm), only a representative picture is shown for each group. Most of the Nrf2-positive cells were detected in D, E and F, a few of Nrf2-positive cells were detected in B and C, and no Nrf2 positive cells were detected in A.

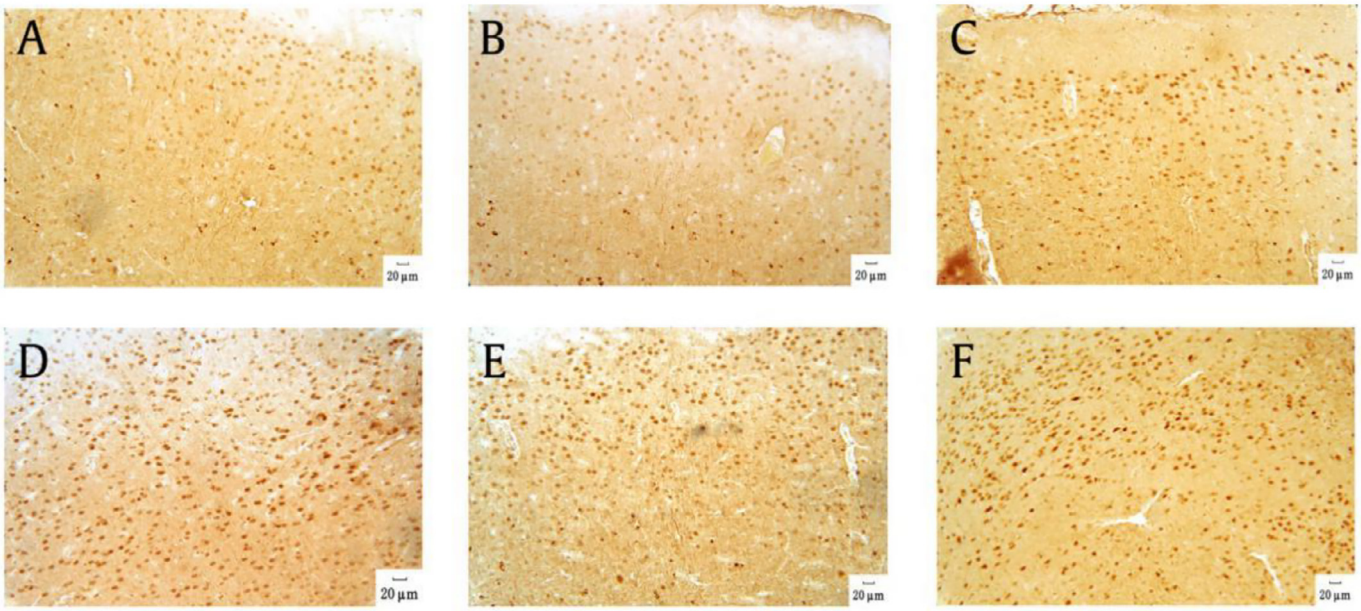

Fig. 10. Effects of MGN on γ-GCS protein expressions shown by IHC detection in brain of experimental rats. (A) Normal; (B) Model; (C) DMSA; (D) MGN 50 mg/kg; (E) MGN 100 mg/kg; (F) MGN 200 mg/kg. At the last day of experiment, 3 male and 3 female rats randomly selected in each group were sacrificed and then their brains were collected as described in Materials and Methods. The expression of γ-GCS in brain tissues was detected by IHC (magnification 200×, scale bars = 20 μm), only a representative picture was shown for each group. γ-GCS positive cells in B were lesser than that in A, but increased in C, and significantly increased in D, E and F.

In our study, the hippocampal histological lesion by HE staining in MGN-treated group was much less severe than that in model group (Fig. 2). Remarkably, MGN blocked the Pb-induced pathological lesions. Hence, MGN may alleviate Pb-induced toxicity.

Oxidative stress has been identified as the primary contributory agent in the pathogenesis of Pb poisoning, while there is ample evidence in support of a very potent antioxidant activity of MGN (Vyas, Syeda, Ahmad, Padhye & Sarkar, 2012). The primary antioxidant mechanisms of MGN seems to be mediated through enhancing GSH levels (Wei, Yan, Deng & Deng, 2011), inhibiting lipid peroxidation (Satish Rao, Sreedevi & Nageshwar Rao, 2009), modulating mitochondrial membrane potential (Lemus-Molina et al., 2009), as well as scavenging ROS (Viswanadh, Rao & Rao, 2010). In this study, supplementation of MGN after Pb exposure resulted in the induction of a scope of antioxidant enzymes, phase II enzymes (HO-1, NQO1, GST), the GSH-related modulating enzyme (γ-GCS) and GSH replenishment in a dose dependent fashion in MGN-treated groups (Figs. 4–6). These findings demonstrated that MGN supplementation maintained a favorable balance between protective antioxidants and potentially harmful oxidants.

The series of genes, as aforementioned, GSH, HO-1 and NQO1, governed by Nrf2, participates in neuroprotection through their own properties (Kwon et al., 2012; Yang et al., 2015). As Nrf2 is the common upstream transcription factor (Sun et al., 2016), the modulatory effects of MGN on the Nrf2 pathway were further evaluated to clarify their preventive functions against Pb-induced neurotoxicities.

We have selectively tested mRNA and protein expression of Nrf2, γ-GCS, HO-1, and also tested the protein expression of Nrf2, γ-GCS by IHC to further study whether these enzyme activities were affected by the expression of Nrf2, γ-GCS and HO-1 genes.

It was observed that mRNA of GCLC, corresponding gene of γ-GCS, together with HO-1 improved statistically significantly in MGN-treated groups, and the levels of Nrf2 mRNA were not increased significantly (Fig. 7(A)). The protein expression levels of Nrf2, HO-1 and γ-GCS were significantly increased in the brain homogenate in MGN-treated group (Fig. 8) and Nrf2 protein expression was significantly increased in nucleus (Fig. 9). The expression of related genes is consistent with that of protein. Thus, it was implied that MGN could effectively activate the Nrf2 pathway to induce the expression of the antioxidative enzymes, phase II enzymes (HO-1, NQO1, and GST) and the GSH-related modulating enzyme.

Our findings showed that IHC, MGN notably promoted the translocation of Nrf2 from the cytoplasm to the nucleus (Fig. 9). In IHC and Western blot, Nrf2 mainly localized in the nucleus (Fig. 9), most of Nrf2-positive cells were detected in MGN-treated groups, a few of Nrf2-positive cells were detected in model group and DMSA-treated group, and no Nrf2-positive cells were detected in normal group (Fig. 9). It indicated that Nrf2 could be activated by Pb, while MGN can further activate it, enhance the accumulation of Nrf2 inside the nucleus without affecting the amount of that in cytoplasm. It was consistent with recent findings (Nguyen, Nioi & Pickett, 2009; Stewart, Killeen, Naquin, Alam, & Alam, 2003).

Nrf2 is a substrate of the protein kinase associated with the MAPK/ERK (extracellular signal-regulated kinase) signaling cascade (Zipper & Mulcahy, 2000). The MAPK cascade, protein kinase C (PKC), and phosphatidylinositol 3-kinase (PI3K) are involved in the activation of Nrf2-Keap1 (Kelch-like ECH-associated protein 1) with a functionally significant cross talk (Su et al., 2013; Wei, Yan, Deng & Deng, 2011). Yao et al. (2012) had reported in this kind of activation, the increased protein expression was due to Nrf2-Keap1 uncoupling, the regulation may not be based on the level of gene transcription, but may be in the post-transcriptional level.

From the results mentioned above, we have concluded that MGN exerts neuroprotective activity against Pb-induced toxicity and oxidative stress via Nrf2 pathways. However, it is still unclear how MGN induced the expression of Nrf2 protein, and further study is required to interpret the mechanism. The schematic

diagram of the Nrf2 signaling pathway and the possible mechanism is as indicated in Fig. 11.

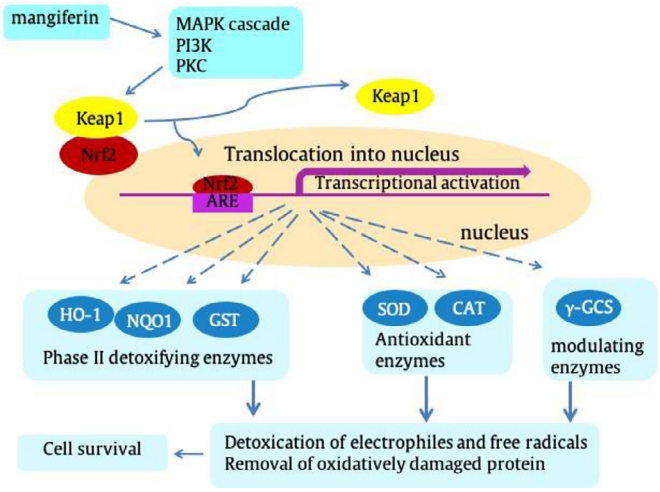

Fig. 11. Schematic diagram of Nrf2/ARE signaling pathway and possible mechanism.

5. Conlusion

In conclusion, our studies have shown that MGN ameliorated morphological damage in the hippocampus. Its neuroprotective effects were achieved by the activation of the Nrf2 downstream genes such as antioxidant enzymes, phase II detoxification enzymes and GSH related enzymes. The data from this *in vitro* study indicates that MGN targeting Nrf2 activation is a feasible approach to reduce adverse health effects associated with Pb exposure. Thus, MGN could be an effective candidate agent for the Pb-induced oxidative stress and neurotoxicity in the human body.

Declaration of Competing Interest

The authors declare no conflict of interests.

Acknowledgments

We are grateful to Dr. Hongwei Guo (Guangxi Meidcal University, China) for discussions and critical comments on the manuscript.

This study was supported by grants from Guangxi Natural Science Foundation Program (No. 2014GXNSFBA118153); Science and Technology Basic Condition Platform of Guangxi Zhuang Autonomous Region, Republic of China (No. 10-046-04); Natural Science Foundation of Guangxi University of Chinese Medicine (No. 2015MS016); Guangxi Natural Science Foundation Program (Nos. 2016GXNSFBA380200, 2016JJA140513).

References

Aoyama, K., Watabe, M., & Nakaki, T. (2008). Regulation of neuronal glutathione synthesis. *Journal of Pharmacological Sciences, 108*(3), 227–238.

Bock, K. W. (2012). Ah receptor- and Nrf2-gene battery members: Modulators of quinone-mediated oxidative and endoplasmic reticulum stress. *Biochemical Pharmacology, 83*(7), 833–838.

Cho, H. Y., Reddy, S. P., Debiase, A., Yamamoto, M., & Kleeberger, S. R. (2005). Gene expression profiling of NRF2-mediated protection against oxidative injury. *Free Radical Biology and Medicine, 38*(3), 325–343.

Dar, A., Faizi, S., Naqvi, S., Roome, T., Zikr-ur-Rehman, S., Ali, M., et al. (2005). Analgesic and antioxidant activity of mangiferin and its derivatives: The structure activity relationship. *Biological & Pharmaceutical Bulletin, 28*(4), 596–600.

Das, J., Ghosh, J., Roy, A., & Sil, P. C. (2012). Mangiferin exerts hepatoprotective activity against D-galactosamine induced acute toxicity and oxidative/nitrosative stress via nrf2-nfkappab pathways. *Toxicology and Applied Pharmacology, 260*(1), 35–47.

Duang, X. Y., Wang, Q., Zhou, X. D., & Huang, D. M. (2011). Mangiferin: A possible strategy for periodontal disease to therapy. *Medical Hypotheses, 76*(4), 486–488.

Flora, G., Gupta, D., & Tiwari, A. (2012). Toxicity of lead: A review with recent updates. *Interdisciplinary Toxicology, 5*(2), 47–58.

Flora, S. J., Saxena, G., & Mehta, A. (2007). Reversal of lead-induced neuronal apoptosis by chelation treatment in rats: Role of reactive oxygen species and intracellular ca^{2+}. *Journal of Pharmacology and Experimental Therapeutics, 322*(1), 108–116.

Garcia-Nino, W. R., & Pedraza-Chaverri, J. (2014). Protective effect of curcumin against heavy metals-induced liver damage. *Food and Chemical Toxicology, 69*, 182–201.

Gottlieb, M., Leal-Campanario, R., Campos-Esparza, M. R., Sanchez-Gomez, M. V., Alberdi, E., Arranz, A., et al. (2006). Neuroprotection by two polyphenols following excitotoxicity and experimental ischemia. *Neurobiology of Disease, 23*(2), 374–386.

Guha, S., Ghosal, S., & Chattopadhyay, U. (1996). Antitumor, immunomodulatory and anti-HIV effect of mangiferin, a naturally occurring glucosylxanthone. *Chemotherapy, 42*(6), 443–451.

Gurer, H., & Ercal, N. (2000). Can antioxidants be beneficial in the treatment of lead poisoning. *Free Radical Biology and Medicine, 29*(10), 927–945.

Han, J., Wang, M., Jing, X., Shi, H., Ren, M., & Lou, H. (2014). (-)-Epigallocatechin gallate protects against cerebral ischemia-induced oxidative stress via nrf2/are signaling. *Neurochemical Research, 39*(7), 1292–1299.

Harder, B., Jiang, T., Wu, T., Tao, S., Rojo de la Vega, M., Tian, W., et al. (2015). Molecular mechanisms of nrf2 regulation and how these influence chemical modulation for disease intervention. *Biochemical Society Transactions, 43*(4), 680–686.

Haskew-Layton, R. E., Payappilly, J. B., Smirnova, N. A., Ma, T. C., Chan, K. K., & Murphy, T. H. (2010). Controlled enzymatic production of astrocytic hydrogen peroxide protects neurons from oxidative stress via an nrf2-independent pathway. *Proceedings of the National Academy of Sciences of the United States of America, 107*(40), 17385–17390.

Hayes, J. D., McMahon, M., Chowdhry, S., & Dinkova-Kostova, A. T. (2010). Cancer chemoprevention mechanisms mediated through the keap1-Nrf2 pathway. *Antioxid Redox Signal, 13*(11), 1713–1748.

He, L., Poblenz, A. T., Medrano, C. J., & Fox, D. A. (2000). Lead and calcium produce rod photoreceptor cell apoptosis by opening the mitochondrial permeability transition pore. *Journal of Biological Chemistry, 275*(16), 12175–12184.

Hsu, P. C., & Guo, Y. L. (2002). Antioxidant nutrients and lead toxicity. *Toxicology, 180*(1), 33–44.

Ibarretxe, G., Sanchez-Gomez, M. V., Campos-Esparza, M. R., Alberdi, E., & Matute, C. (2006). Differential oxidative stress in oligodendrocytes and neurons after excitotoxic insults and protection by natural polyphenols. *Glia, 53*(2), 201–211.

Ikram, M., Muhammad, T., Rehman, S. U., Khan, A., Jo, M. G., Ali, T., et al. (2019). Hesperetin confers neuroprotection by regulating nrf2/tlr4/nf-kappab signaling in an abeta mouse model. *Molecular Neurobiology, 56*(9), 6293–6309.

Janaky, R., Varga, V., Hermann, A., Saransaari, P., & Oja, S. S. (2000). Mechanisms of L-cysteine neurotoxicity. *Neurochemical Research, 25*(9–10), 1397–1405.

Jo, G. H., Kim, G.-. Y., Kim, W.-. J., Park, K. Y., & Choi, Y. H. (2014). Sulforaphane induces apoptosis in T24 human urinary bladder cancer cells through a reactive oxygen species-mediated mitochondrial pathway: The involvement of endoplasmic reticulum stress and the nrf2 signaling pathway. *International Journal of Oncology, 25*(4), 1497–1506.

Khurana, R. K., Kaur, R., Lohan, S., Singh, K. K., & Singh, B. (2016). Mangiferin: A promising anticancer bioactive. *Pharmaceutical patent analyst, 5*(3), 169–181.

Kwon, J., Han, E., Bui, C. B., Shin, W., Lee, J., Lee, S., et al. (2012). Assurance of mitochondrial integrity and mammalian longevity by the p62-Keap1-Nrf2-Nqo1 cascade. *Embo Reports, 13*(2), 150–156.

Lemus-Molina, Y., Sanchez-Gomez, M. V., Delgado-Hernandez, R., & Matute, C. (2009). Mangifera indica L. extract attenuates glutamate-induced neurotoxicity on rat cortical neurons. *Neurotoxicology, 30*(6), 1053–1058.

Li, H. W., Deng, J. G., Du, Z. C., Yan, M. S., Long, Z. X., Pham Thi, P. T., et al. (2013). Protective effects of mangiferin in subchronic developmental lead-exposed rats. *Biological Trace Element Research, 152*(2), 233–242.

Liu, B., Zhang, H., Tan, X., Yang, D., Lv, Z., Jiang, H., et al. (2017). GSPE reduces lead-induced oxidative stress by activating the nrf2 pathway and suppressing miR153 and GSK-3beta in rat kidney. *Oncotarget, 8*(26), 42226–42237.

Liu, H., Feng, Y., Xu, M., Yang, J., Wang, Z., & Di, G. (2018). Four-octyl itaconate activates keap1-nrf2 signaling to protect neuronal cells from hydrogen peroxide. *Cell Communication and Signaling, 16*(1), 81.

Loboda, A., Damulewicz, M., Pyza, E., Jozkowicz, A., & Dulak, J. (2016). Role of nrf2/ho-1 system in development, oxidative stress response and diseases: An evolutionarily conserved mechanism. *Cellular and Molecular Life Sciences, 73*(17), 3221–3247.

Lopes, A. C., Peixe, T. S., Mesas, A. E., & Paoliello, M. M. (2016). Lead exposure and oxidative stress: A systematic review. *Reviews of Environmental Contamination and Toxicology, 236*, 193–238.

Lou, Y., Guo, Z., Zhu, Y., Kong, M., Zhang, R., Lu, L., et al. (2019). Houttuynia cordata thunb. and its bioactive compound 2-undecanone significantly suppress benzo(a)pyrene-induced lung tumorigenesis by activating the nrf2-ho-1/nqo-1 signaling pathway. *Journal of Experimental & Clinical Cancer Research, 38*(1), 242.

Lu, J., Jiang, H., Liu, B., Baiyun, R., Li, S., Lv, Y., et al. (2018). Grape seed procyanidin extract protects against pb-induced lung toxicity by activating the AMPK/Nrf2/p62 signaling axis. *Food and Chemical Toxicology, 116*(Pt B), 59–69.

Luczkiewicz, P., Kokotkiewicz, A., Dampc, A., & Luczkiewicz, M. (2014). Mangiferin: A promising therapeutic agent for rheumatoid arthritis treatment. *Medical Hypotheses, 83*(5), 570–574.
Mahalanobish, S., Saha, S., Dutta, S., & Sil, P. C. (2019). Mangiferin alleviates arsenic induced oxidative lung injury via upregulation of the nrf2-ho1 axis. *Food and Chemical Toxicology, 126*, 41–55.
Martinez-Lazcano, J. C., Lopez-Quiroz, A., Alcantar-Almaraz, R., Montes, S., Sanchez–Mendoza, A., Alcaraz-Zubeldia, M., et al. (2018). A hypothesis of the interaction of the nitrergic and serotonergic systems in aggressive behavior induced by exposure to lead. *Frontiers in Behavioral Neuroscience, 12*, 202.
Motohashi, H., & Yamamoto, M. (2004). Nrf2-Keap1 defines a physiologically important stress response mechanism. *Trends in Molecular Medicine, 10*(11), 549–557.
Nguyen, T., Nioi, P., & Pickett, C. B. (2009). The nrf2-antioxidant response element signaling pathway and its activation by oxidative stress. *Journal of Biological Chemistry, 284*(20), 13291–13295.
Nyqvist, F., Helmfrid, I., Augustsson, A., & Wingren, G. (2017). Increased cancer incidence in the local population around metal-contaminated glassworks sites. *Journal of Occupational and Environmental Medicine, 59*(5), e84–e90.
Pal, P. B., Sinha, K., & Sil, P. C. (2013). Mangiferin, a natural xanthone, protects murine liver in pb(ii) induced hepatic damage and cell death via map kinase, nf-kappab and mitochondria dependent pathways. *Plos One, 8*(2), e56894.
Pardo Andreu, G. L., Maurmann, N., Reolon, G. K., de Farias, C. B., Schwartsmann, G., Delgado, R., et al. (2010). Mangiferin, a naturally occurring glucoxilxanthone improves long-term object recognition memory in rats. *European Journal of Pharmacology, 635*(1–3), 124–128.
Patrick, L. (2006). Lead toxicity part II: The role of free radical damage and the use of antioxidants in the pathology and treatment of lead toxicity. *Alternative Medicine Review : A Journal of Clinical Therapeutic, 11*(2), 114–127.
Peng, S., Hou, Y., Yao, J., & Fang, J. (2019). Neuroprotection of mangiferin against oxidative damage via arousing Nrf2 signaling pathway in PC12 cells. *BioFactors (Oxford, England), 45*(3), 381–392.
Raza, H. (2011). Dual localization of glutathione S-transferase in the cytosol and mitochondria: Implications in oxidative stress, toxicity and disease. *The Febs Journal, 278*(22), 4243–4251.
Roy, A., & Kordas, K. (2016). The relation between low-level lead exposure and oxidative stress: A review of the epidemiological evidence in children and non-occupationally exposed adults. *Current Environmental Health Reports, 3*(4), 478–492.
Rubiolo, J. A., Mithieux, G., & Vega, F. V. (2008). Resveratrol protects primary rat hepatocytes against oxidative stress damage: Activation of the nrf2 transcription factor and augmented activities of antioxidant enzymes. *European Journal of Pharmacology, 591*(1–3), 66–72.
Sadhukhan, P., Saha, S., Dutta, S., & Sil, P. C. (2018). Mangiferin ameliorates cisplatin induced acute kidney injury by upregulating Nrf-2 via the activation of PI3K and exhibits synergistic anticancer activity with cisplatin. *Frontiers in Pharmacology, 9*, 638.
Saha, S., Rashid, K., Sadhukhan, P., Agarwal, N., & Sil, P. C. (2016). Attenuative role of mangiferin in oxidative stress-mediated liver dysfunction in arsenic-intoxicated murines. *BioFactors (Oxford, England), 42*(5), 515–532.
Sakthithasan, K., Levy, P., Poupon, J., & Garnier, R. (2018). A comparative study of edetate calcium disodium and dimercaptosuccinic acid in the treatment of lead poisoning in adults. *Clinical toxicology (Philadelphia, PA.), 56*(11), 1143–1149.
Satish Rao, B. S., Sreedevi, M. V., & Nageshwar Rao, B. (2009). Cytoprotective and antigenotoxic potential of mangiferin, a glucosylxanthone against cadmium chloride induced toxicity in hepg2 cells. *Food and Chemical Toxicology, 47*(3), 592–600.
Scapagnini, G., Vasto, S., Abraham, N. G., Caruso, C., Zella, D., & Fabio, G. (2011). Modulation of nrf2/are pathway by food polyphenols: A nutritional neuroprotective strategy for cognitive and neurodegenerative disorders. *Molecular Neurobiology, 44*(2), 192–201.
Singh, G., Singh, V., Wang, Z. X., Voisin, G., Lefebvre, F., & Navenot, J. M. (2018). Effects of developmental lead exposure on the hippocampal methylome: Influences of sex and timing and level of exposure. *Toxicology Letters, 290*, 63–72.
Slocum, S. L., & Kensler, T. W. (2011). Nrf2: Control of sensitivity to carcinogens. *Archives of Toxicology, 85*(4), 273–284.
Stewart, D., Killeen, E., Naquin, R., Alam, S., & Alam, J. (2003). Degradation of transcription factor nrf2 via the ubiquitin-proteasome pathway and stabilization by cadmium. *Journal of Biological Chemistry, 278*(1), 2396–2402.
Su, P., Zhang, J., Wang, S., Aschner, M., Cao, Z., Zhao, F., et al. (2016). Genistein alleviates lead-induced neurotoxicity *in vitro* and *in vivo*: Involvement of multiple signaling pathways. *Neurotoxicology, 53*, 153–164.
Su, Z. Y., Shu, L., Khor, T. O., Lee, J. H., Fuentes, F., & Kong, A. N. (2013). A perspective on dietary phytochemicals and cancer chemoprevention: Oxidative stress, nrf2, and epigenomics. *Topics in Current Chemistry, 329*, 133–162.
Sun, Y., Liu, J., Wan, L., Wang, F., Zhang, X. J., & Qi, Y. J. (2016). Improving effects of *astragalus* polysaccharides on cardiac function via keap1/nrf2-are signal pathway in adjuvant arthritis rats. *Chinese Herbal Medicines, 8*(2), 143–153.
Talalay, P., Fahey, J. W., Holtzclaw, W. D., Prestera, T., & Zhang, Y. (1995). Chemoprotection against cancer by phase 2 enzyme induction. *Toxicology Letters, 82-83*, 173–179.
Thimmulappa, R. K., Mai, K. H., Srisuma, S., Kensler, T. W., Yamamoto, M., & Biswal, S. (2002). Identification of nrf2-regulated genes induced by the chemopreventive agent sulforaphane by oligonucleotide microarray. *Cancer Research, 62*(18), 5196–5203.
Tin, O. K., Huang, Y., Wu, T.-Y., Shu, L., Lee, J., Kong, T., & Ng, A. (2011). Pharmacodynamics of curcumin as dna hypomethylation agent in restoring the expression of nrf2 via promoter cpgs demethylation. *Biochemical Pharmacology, 82*(9), 1073–1078.
Viswanadh, E. K., Rao, B. N., & Rao, B. S. (2010). Antigenotoxic effect of mangiferin and changes in antioxidant enzyme levels of swiss albino mice treated with cadmium chloride. *Human & Experimental Toxicology, 29*(5), 409–418.
Vorvolakos, T., Arseniou, S., & Samakouri, M. (2016). There is no safe threshold for lead exposure: Alpha literature review. *Psychiatrike, 27*(3), 204–214.
Vyas, A., Syeda, K., Ahmad, A., Padhye, S., & Sarkar, F. H. (2012). Perspectives on medicinal properties of mangiferin. *Mini Reviews in Medicinal Chemistry, 12*(5), 412–425.
Wagner, P. J., Park, H. R., Wang, Z., Kirchner, R., Wei, Y., Su, L., et al. (2017). *In vitro* effects of lead on gene expression in neural stem cells and associations between up-regulated genes and cognitive scores in children. *Environmental Health Perspectives, 125*(4), 721–729.
Wang, Y. J., Wang, X. Y., Hao, X. Y., Yan, Y. M., Hong, M., Wei, S. F., et al. (2019). Ethanol extract of *centipeda minima* exerts antioxidant and neuroprotective effects via activation of the nrf2 signaling pathway. *Oxidative Medicine and Cellular Longevity, 2019*, 9421037.
Wang, Z., Guo, S., Wang, J., Shen, Y., Zhang, J., & Wu, Q. (2017). Nrf2/HO-1 mediates the neuroprotective effect of mangiferin on early brain injury after subarachnoid hemorrhage by attenuating mitochondria-related apoptosis and neuroinflammation. *Scientific Reports, 7*(1), 11883.
Wei, Z. Q., Deng, J. G., & Yan, L. (2011a). Pharmacological effects of mangiferin. *Chinese Herbal Medicines, 3*(4), 266–271.
Wei, Z. Q., Yan, L., Deng, J. G., & Deng, J. (2011b). Effects of mangiferin on mapk signaling pathway in chronic inflammation. *Zhongguo Zhong yao za zhi China Journal of Chinese materia medica, 36*(13), 1798–1802.
Winiarska-Mieczan, A. (2018). Protective effect of tea against lead and cadmium-induced oxidative stress-a review. *Biometals: An International Journal on the Role of Metal Ions in Biology, Biochemistry, and Medicine, 31*(6), 909–926.
Xia, G., Li, X., Zhu, X., Yin, X., Ding, H., & Qiao, Y. (2017). Mangiferin protects osteoblast against oxidative damage by modulation of ERK5/Nrf2 signaling. *Biochemical and Biophysical Research Communications, 491*(3), 807–813.
Yang, M. Y., Yu, Q. L., Huang, Y. S., & Yang, G. (2019). Neuroprotective effects of andrographolide derivative CX-10 in transient focal ischemia in rat: Involvement of nrf2/ae and tlr/nf-kappab signaling. *Pharmacological Research, 144*, 227–234.
Yang, Y., Jiang, S., Yan, J., Li, Y., Xin, Z., Lin, Y., et al. (2015). An overview of the molecular mechanisms and novel roles of nrf2 in neurodegenerative disorders. *Cytokine & Growth Factor Reviews, 26*(1), 47–57.
Yang, Z., Weian, C., Susu, H., & Hanmin, W. (2016). Protective effects of mangiferin on cerebral ischemia-reperfusion injury and its mechanisms. *European Journal of Pharmacology, 771*, 145–151.
Yao, J. W., Liu, J., Kong, X. Z., Zhang, S. G., Wang, X. H., Yu, M., et al. (2012). Induction of activation of the antioxidant response element and stabilization of Nrf2 by 3-(3-pyridylmethylidene)-2-indolinone (PMID) confers protection against oxidative stress-induced cell death. *Toxicology and Applied Pharmacology, 259*(2), 227–235.
Yao, J., Peng, S., Xu, J., & Fang, J. (2019). Reversing ROS-mediated neurotoxicity by chlorogenic acid involves its direct antioxidant activity and activation of Nrf2-are signaling pathway. *BioFactors (Oxford, England), 45*(4), 616–626.
Ye, F., Li, X., Li, L., Yuan, J., & Chen, J. (2016). t-BHQ provides protection against lead neurotoxicity via Nrf2/ho-1 pathway. *Oxidative Medicine and Cellular Longevity, 2016*, 2075915.
Zhang, B., Zhao, J., Li, S., Zeng, L., Chen, Y., & Fang, J. (2015). Mangiferin activates the nrf2-are pathway and reduces etoposide-induced dna damage in human umbilical cord mononuclear blood cells. *Le Pharmacien Biologiste, 53*(4), 503–511.
Zhang, C., Su, Z. Y., Khor, T. O., Shu, L., & Kong, A. N. (2013). Sulforaphane enhances Nrf2 expression in prostate cancer tramp C1 cells through epigenetic regulation. *Biochemical Pharmacology, 85*(9), 1398–1404.
Zhou, Y., Wang, H. D., Zhou, X. M., Fang, J., Zhu, L., & Ding, K. (2018). *N*-acetylcysteine amide provides neuroprotection via Nrf2-are pathway in a mouse model of traumatic brain injury. *Drug Design, Development and Therapy, 12*, 4117–4127.
Zipper, L. M., & Mulcahy, R. T. (2000). Inhibition of Erk and p38 map kinases inhibits binding of Nrf2 and induction of GCS genes. *Biochemical and Biophysical Research Communications, 278*(2), 484–492.
WHO. (2017). WHO Model Lists of Essential Medicines. Retrieved from https://www.who.int/medicines/publications/essentialmedicines/en/.